Title: Retrograde Axonal Transport of BDNF and proNGF Diminishes with Age in Basal Forebrain Cholinergic Neurons

Authors: Arman Shekari[a], Margaret Fahnestock[a]

[a] Department of Psychiatry and Behavioural Neurosciences, McMaster University, 1280 Main St. West, Hamilton, Ontario L8S 4K1, Canada

Corresponding author:

Margaret Fahnestock, Ph.D.

Department of Psychiatry & Behavioural Neurosciences

McMaster University

1280 Main Street West

Hamilton, ON L8S 4K1, Canada

Tel. 1-905-525-9140, ext. 23344

Fax 1-905-522-8804

E-mail fahnest@mcmaster.ca

Declarations of interest: none.

Highlights:

- BDNF and proNGF transport are reduced in basal forebrain neurons with aging *in vitro*
- BDNF transport is impaired in aged basal forebrain compared to cortical neurons
- TrkA and TrkB levels are reduced with aging, but p75NTR levels are maintained
- Age-induced transport deficits may contribute to neurodegeneration in Alzheimer's

Abstract: Basal forebrain cholinergic neurons (BFCNs) are critical for learning and memory and degenerate early in Alzheimer's disease. BFCNs depend for their survival and function on nerve growth factor (NGF) and brain-derived neurotrophic factor (BDNF) which are retrogradely transported from BFCN targets. Age is the greatest risk factor for developing Alzheimer's disease, yet the influence of age on BFCN axonal transport is poorly understood. To model aging, embryonic rat basal forebrain or cortical neurons were cultured in microfluidic chambers. Staining for senescence-associated beta-galactosidase indicated an aging phenotype and was observed only in BFCNs cultured for 18 or more days *in vitro.* Significant reductions in BDNF transport speed and increases in pause duration were seen in aged BFCNs but not cortical neurons. Young BFCNs displayed robust proNGF transport, which also diminished with *in vitro* age. The expression of NGF receptor TrkA and BDNF receptor TrkB also decreased significantly as a function of *in vitro* aging in BFCNs only. These results suggest a unique vulnerability of BFCNs to age-induced transport deficits. These deficits, coupled with the reliance of BFCNs on axonal transport of neurotrophins, may explain their vulnerability to age-related disorders like Alzheimer's disease.

Key words: axonal transport, neurotrophins, neurodegeneration, basal forebrain, Alzheimer's disease, Trk receptors

Abbreviations: AD: Alzheimer's Disease; APP: Amyloid precursor protein; BDNF: brain derived neurotrophic factor; BFCN: Basal forebrain cholinergic neuron; DIV: Days *in vitro;* DMEM: Dulbecco's Minimal Essential Medium; DRG: dorsal root ganglion; HBSS: Hank's Balanced Salt Solution; LHX-7: Lim homebox-7; MAPK: Mitogen-activated protein kinase; NGF: Nerve growth factor; PBS: phosphate-buffered saline; QD: quantum dot; SaβG: senescence-associated beta-galactosidase; TrkA: tropomyosin-related kinase A; TrkB: tropomyosin-related kinase B; VAChT: vesicular acetylcholine transporter

Acknowledgements: The authors are grateful to Drs. Wayne Poon and Carl Cotman (UC Irvine) and Dr. Chengbiao Wu (UCSD) for help with microfluidic chambers and transport assays.

Funding: Supported by grants to MF from the Alzheimer Society of Canada and the Canadian Institutes of Health Research (MOP-102723, PJT-159493), and by an Ontario Graduate Scholarship to AS.

1. **Introduction**

The basal forebrain is the primary source of cholinergic innervation in the central nervous system (CNS) and plays a critical role in learning, memory, attention and regulation of cortical blood flow (Ballinger et al., 2016; Baxter and Chiba, 1999; Linville and Arnerić, 1991). Diffuse projections from basal forebrain cholinergic neurons (BFCNs) terminate mainly in the hippocampus and throughout the cortex (Ballinger et al., 2016). These projections, especially those of the septohippocampal tract, have been shown to degenerate with age (Grothe et al., 2012; Ypsilanti et al., 2008). ~~Extreme and rapid~~ Degeneration of the basal forebrain has been repeatedly observed in age-related neurodegenerative disorders like Alzheimer's disease (AD), with multiple studies demonstrating that basal forebrain dysfunction is predictive of the disorder (Baker-Nigh et al., 2015; Ballinger et al., 2016; Schmitz et al., 2016; Teipel et al., 2014). Furthermore, synaptic loss in BFCNs correlates strongly with dementia severity in AD and is implicated in aging and age-associated memory deficits (Ballinger et al., 2016; H. Ferreira-Vieira et al., 2016; Whitehouse et al., 1982; Ypsilanti et al., 2008).

Age-related degeneration of BFCNs may occur due to their unique reliance on target-derived trophic support. BFCNs do not make their own neurotrophins. They rely on their cortical and hippocampal targets to produce brain-derived neurotrophic factor (BDNF) and nerve growth factor (NGF) that are transported back to BFCN cell bodies via retrograde axonal transport (DiStefano et al., 1992; Götz et al., 2001; Seiler and Schwab, 1984; Sobreviela et al., 1996). Neurotrophins like BDNF and NGF are critical for a wide variety of cellular processes including apoptotic suppression, differentiation, activity-dependent plasticity and maintenance of synaptic connectivity (Bothwell, 2014). As a result, retrograde axonal transport of neurotrophins by BFCNs is crucial for their proper function and survival. NGF receptor alterations have been observed prior to phenotypic alteration of BFCNs in AD, suggesting that a lack of neurotrophic support is causative with respect to basal forebrain degeneration (Mufson et al., 2003, 2000). In postmortem AD BFCN, tropomyosin-related kinase A (TrkA) receptor is lost while the pan-neurotrophin receptor $p75^{NTR}$ and tropomyosin-related kinase B (TrkB) receptors are stable

(Counts et al., 2004; Ginsberg et al., 2006; Mufson et al., 2000). Increased NGF-like immunoreactivity has been found in both the AD cortex and hippocampus, with decreased levels in the basal forebrain, suggesting a deficit in retrograde axonal NGF transport (Scott et al., 1995). Impaired NGF transport in BFCNs has also been demonstrated in the amyloid precursor protein (APP) overexpressing Ts65Dn Down syndrome mouse model (Cooper et al., 2001; Salehi et al., 2006). These results implicate dysfunctional BFCN retrograde axonal transport in AD pathogenesis.

Aside from AD, age itself has been shown to negatively impact the basal forebrain. BFCN nuclear size and overall BFCN numbers are decreased in aged rats (Altavista et al., 1990). TrkA receptor levels, the receptor for NGF, and levels of downstream NGF signaling proteins are decreased in aged rat BFCNs (Parikh et al., 2013; Williams et al., 2007, 2006). The length of cholinergic fibers projecting to the hippocampus from the basal forebrain is reduced with age (Ypsilanti et al., 2008). Moreover, general retrograde axonal transport is diminished in aged rat BFCNs (Bearer et al., 2018; Cooper et al., 1994; De Lacalle et al., 1996). These deficits have behavioral consequences, as both aged rats and Lim Homebox-7 (LHX7) knockout mice that fail to develop forebrain cholinergic neurons show learning and memory impairments (Fragkouli et al., 2005; Gustilo et al., 1999).

~~The retrograde axonal transport of BDNF and NGF is critical to BFCNs due to their lack of neurotrophin autocrine production.~~ While aging has been demonstrated to impact general axonal transport in the basal forebrain, the impact of aging on neurotrophin-specific transport is poorly understood. Although both proBDNF and BDNF are found in the CNS (Michalski & Fahnestock, 2003), the form of NGF found in both human and rodent brain is proNGF (Fahnestock et al., 2001). ProNGF binds to TrkA and activates MAPK and Akt pathways to signal survival and neurite outgrowth (Fahnestock et al., 2004; Clewes et al., 2008; Ioannou and Fahnestock, 2017; Masoudi et al., 2009; Fahnestock & Shekari, 2019). ProNGF is retrogradely transported by peripheral dorsal root ganglion neurons (DRGs) and co-localizes with TrkA and $p75^{NTR}$ in DRG axons (De Nadai et al., 2016). However, proNGF axonal transport in the CNS has not been reported in the literature. BDNF retrograde transport has been demonstrated in both

cortical and hippocampal neurons, but not in BFCNs (Poon et al., 2011; Zhao et al., 2014). As a result, we sought to explore the impact of age on proNGF and BDNF axonal transport in BFCNs.

To study transport in BFCNs, we adopted a microfluidic platform to separate neuronal cell bodies from axons. To model aging, cells were assayed after either 7-10 days *in vitro* (DIV), just enough time to allow axons to cross the 450μM microgroove barrier, or 18-20 DIV. Aging *in vitro* is not a perfect analog of *in vivo* aging, but is commonly used in both primary neuron and stem cell cultures to examine age-sensitive phenomena (Campos et al., 2014; Martin et al., 2008; Palomer et al., 2016; Sodero et al., 2011; Uday Bhanu et al., 2010). To confirm an aging phenotype in our neurons, BFCNs were stained with senescence-associated beta galactosidase (SaβG), a well-validated marker of aging in humans, primates, and rodents both *in vivo* and *in vitro* (Dimri et al., 1995; Kurz et al., 2000; Mishima et al., 1999; Uday Bhanu et al., 2010).

2. **Methods**

All reagents were purchased from ThermoFisher Scientific (Burlington, ON, Canada) unless otherwise stated.

2.1 *Neuron Culture in Microfluidic Chambers*

One day prior to dissection, microfluidic chambers (Xona Microfluidics, Temecula, California) were prepared according to the manufacturer's instruction. Briefly, 95% ethanol was added to each well of the chamber, followed by two phosphate-buffered saline (PBS) washes. 100µL of poly-L-lysine (Sigma Aldrich, Burlington, Ontario) was added to each of the wells, and the chambers were left to incubate overnight in a 37°C, 5% CO_2 incubator. The chambers were then washed once with PBS, and 150uL of cell culture medium was added to each of the wells. The cell culture medium consisted of Neurobasal, 1% Penicillin-Streptomycin, 1X B27 supplement, 1X GlutaMAX supplement, 1% Fetal Bovine Serum, 50ng/mL BDNF (Peprotech, Rocky Hill, New Jersey), and 50 ng/mL NGF (generous gift from Dr. Michael Coughlin, McMaster University, Hamilton, Canada). The chambers were left to incubate at 37°C 5% CO_2 during the dissection.

Whole basal forebrain and cortex were dissected from embryonic day 18 (E18) rat embryos and immediately placed on ice in a solution of Hank's Balanced Salt Solution (HBSS) with 1% Penicillin-Streptomycin. The tissue from 5 embryos was pooled for each round of dissection, therefore sex was not determined. The neural tissue was washed with fresh HBSS five times and then trypsinized in a 37°C water bath for 20 minutes. DNase I (Sigma Aldrich) was added to a final concentration of 1X, and the tissue was triturated using a sterile, small-bore, fire-polished, glass pipette. 1mL of cell culture medium was then added, and the suspension was centrifuged at 250xg for 4 minutes. The cell pellet was resuspended in 300uL of cell culture medium, and the volume was adjusted to a final concentration of 1.0 x 10^6 cells/mL. 140uL of medium was removed from each of the four wells of the chambers, and 10uL of cell suspension was added to the two left wells. The chambers were incubated for 10 minutes to allow cell

adherence, which was confirmed under a microscope (Zeiss AxioVert A1). 150uL of cell culture medium was then added to all wells, and the cells were incubated overnight at 37°C and 5% CO_2. The next day, all the medium was removed and replaced with a serum-free variant of the medium described above. Cells were maintained in this medium for the duration of the experiments, with medium changes occurring every 48-72 hours.

2.2 *Immunostaining and Confirmation of BFCN Phenotype.*

Neurons were stained for TrkA, TrkB, $p75^{NTR}$, and vesicular acetylcholine transporter (VAChT). Immunostaining was carried out in the microfluidic devices themselves. Cells were fixed in freshly prepared 4% paraformaldehyde for 30 minutes at room temperature (RT). Cells were washed twice with PBS, permeabilized with 0.2% Triton-X100 in PBS for 30 minutes at RT and blocked with 3% bovine serum albumin in PBS for 30 minutes at RT. Primary antibodies anti-TrkA (Santa Cruz Biotechnology, Santa Cruz, California) or anti-VAChT (Santa Cruz Biotechnology, Santa Cruz, California) were added at a 1:500 dilution, anti-TrkB (Cell Signaling Technologies, Danvers, Massachusetts) at a 1:500 dilution, and anti-$p75^{NTR}$ (Cell Signaling Technologies, Danvers, Massachusetts) at a 1:1600 dilution and were left to incubate overnight at 4°C. Cells were washed with blocking solution 3 times on the following day. Alexa Fluor 488 secondary antibody was then added at a 1:1000 dilution and was left to incubate for 2 hours at RT. Neurons were visualized via fluorescence microscopy using a YFP filter cube set (488nm excitation, 525nm emission). All immunostaining was carried out in microfluidic chambers between DIV 10-18. TrkA and VAChT staining was robust at DIV10 (Supplementary Figure 1A, B). Cortical neurons, as expected, did not express either and were used as a negative control (Supplementary Figure 1C).

2.3 *Histological Staining*

Neurons were stained for senescence-associated beta-galactosidase (SaβG) at DIV7-10 and at DIV18-20. Cells were stained within the chambers themselves, with 150uL of fixative added to all wells,

followed by 150uL of staining solution prepared according to the manufacturer's instruction (Cell Signaling, Danvers, Massachusetts). Cells were imaged using a Zeiss AxioVert A1 microscope.

2.4 *Preparation of Labelled Neurotrophins*

2.4.1 *BDNF*

Biotinylated BDNF was purchased from Alomone Labs (Tel Aviv, Israel). BDNF-biotin was incubated with Quantum Dot 625 Streptavidin conjugate at a 1:1 molar ratio on ice for one hour in the dark, and then diluted to 1nM using serum-free cell culture medium without BDNF and NGF.

2.4.2 *proNGF*

We use a cleavage-resistant proNGF mutant containing a cytosine-to-guanine point mutation at position 633, resulting in an arginine-to-glycine substitution at the -1 position (ProNGF[R-1G]; Fahnestock et al., 2004). This cleavage-resistant proNGF binds to TrkA and $p75^{NTR}$, is internalized and activates Mitogen-activated protein kinase (MAPK) and Akt pathways (Fahnestock et al., 2004; Ioannou and Fahnestock, 2017; Masoudi et al., 2009). This sequence was engineered to include both a biotin-accepting AVI region and a nickel-binding histidine tag, as described in (Sung et al., 2011). Briefly, a vector containing mature NGF-avi (a generous gift from Dr. Chengbiao Wu, UCSD) was digested using EcoR1 and BamH1, and the excised NGF-avi fragment was ligated into a PCDNA 3.1 myc.his(+) vector. The R-1G mutation was then introduced using site-directed mutagenesis as described in Fahnestock et al. (2004) using the QuickChange II site-directed mutagenesis kit from Agilent Technologies (Santa Clara, USA).

1ug of the tagged proNGF[R-1G] plasmid, along with 20ug of a plasmid encoding biotin ligase (a generous gift from Dr. Chengbiao Wu, USCD) were co-transfected into HEK293FT cells using Lipofectamine 3000. Cells were grown to 70% confluency in medium containing Dulbecco's Minimal Essential Medium (DMEM), 1% FBS, 1% Penicillin-Streptomycin, 200mM GlutaMAX supplement,

50μM D-biotin (Sigma Aldrich) and 100mM sodium pyruvate (Sigma Aldrich). Medium was collected 72 hours post-transfection. ProNGF-biotin was purified from the medium via nickel affinity chromatography. Protein concentration was determined via an in-house NGF ELISA (Fahnestock et al, 2004). Biotinylated proNGF was shown to be intact by Western blotting (Supplementary Figure 2) and was labeled with Quantum Dot 625 as described above for BDNF.

2.5 *Tracking Neurotrophin Transport*

2.5.1 *BDNF*

Neuronal cell bodies and axons were starved of neurotrophin by incubating overnight in medium containing only Neurobasal, 1% Penicillin-Streptomycin, 1X B27 supplement, and 1X GlutaMAX supplement. The next day, cells were washed 3 times with this neurotrophin-free medium to remove any residual neurotrophins. 160μL of 1nM quantum dot-labeled BDNF (QD-BDNF) was added to the axonal side of the chambers and was incubated for one hour (BFCNs) or 4 hours (cortical neurons) to account for differences in BDNF uptake efficiency between the cell types. The chambers were then transferred to an EVOS2 FL Microscope (ThermoFisher Scientific) with an environmental chamber set to 37°C and 5% CO_2. Quantum dots were visualized using a TexasRed filter, exciting at 585nm and detecting emission at 624nm. Kymographs were generated by compiling 120 images (from the TexasRed filter only) taken every 2 seconds into a vertical Z-stack using ImageJ. Particle speeds and pause duration were calculated using the mTrackJ ImageJ plug-in to track the distance travelled by labelled particles between images. Experiments were repeated three times.

2.5.2 *proNGF*

BFCN cell bodies were starved of neurotrophins as described above, and 160μL of 50pM quantum dot-labeled proNGF (QD-proNGF) was added to the axons and incubated for 1 hour. The same microscope described above was used to capture the proNGF data. Mean fluorescence intensity was

determined by measuring the mean grey value of pixels within proNGF-positive cell bodies with ImageJ. Experiments were repeated 3 times.

2.6 Statistical Analysis

Sample sizes were similar to those reported in other related publications (Mufson et al., 2000; Poon et al., 2011; Zhao et al., 2014). Unpaired, two-tailed Student's t-tests were performed when comparing 2 groups, with a confidence interval of 95%. One-way ANOVA with *post hoc* Tukey tests were performed when more than 2 groups were compared, with a p value of 0.05 being considered significant. All error bars represent the standard error of the mean (SEM). Statistical methods are further elaborated upon in the text and in figure legends.

3. **Results**

3.1 *BDNF Transport is Impaired in Aged BFCNs but not cortical neurons*

To determine the effect of aging *in vitro* on retrograde neurotrophin transport in BFCNs, axonal transport assays using QD-BDNF were carried out and kymographs were generated using neurons kept in culture for differing lengths of time. DIV8 BFCNs (Fig. 1A-C) and DIV22 cortical neurons (Fig. 1G-I) showed robust BDNF transport as indicated by horizontal/diagonal lines in the kymographs, whereas QD-BDNF taken up by DIV21 BFCNs were largely stationary as shown by the vertical lines (Fig. 1D-F). Quantification of BDNF-QD particle movement (Fig. 2A-B) demonstrated that the speed of QD-BDNF particles decreased significantly in DIV18-20 BFCNs compared to DIV7-10 BFCNs (*N*=60 QD-BDNF particles per group, p= 0.003, 1-way ANOVA and *post hoc* Tukey test). However, QD-BDNF particle speed did not differ between DIV7-10 BFCNs and DIV18 cortical neurons (*N*=60 QD-BDNF particles per group p=0.9, 1-way ANOVA and *post hoc* Tukey test). BDNF-QD particles also paused for significantly longer in DIV18-20 BFCNs compared to DIV7-10 BFCNs (N=60 QD-BDNF particles per group, p<0.001, 1-way ANOVA and *post hoc* Tukey test). BDNF-QD particles in DIV18-20 cortical neurons did not differ significantly in pause duration from DIV7-10 BFCNs (N=60 QD-BDNF particles per group, p=0.928, 1-way ANOVA and *post hoc* Tukey test). BDNF transport did not decrease significantly with further *in vitro* aging, as DIV21-24 BFCNs were not significantly different from DIV18-20 BFCNs in terms of BDNF speed and pause duration (data not shown).

3.2 *proNGF Uptake is Robust in Young BFCNs and is Reduced with Age in vitro*

Next, we aimed to characterize proNGF transport in BFCNs and to assess the role of *in vitro* aging on the process. To determine if similar axonal transport deficits could be seen with proNGF, experiments were repeated using the same timepoints with cleavage-resistant proNGF as opposed to BDNF. Of note, cortical neurons could not be used as a comparison group due to their lack of TrkA expression.

The conditions required for proNGF uptake differed from BDNF: neurotrophic starvation of axon terminals and cell bodies, as carried out for BDNF, resulted in no proNGF being taken up by BFCNs; proNGF transport occurred only after cell bodies alone instead of axon terminals and cell bodies were starved of neurotrophins (Fig. 3A-B). We also determined that proNGF uptake by DIV7-10 BFCNs was extremely rapid. ProNGF uptake occurred within 15 minutes of its administration, and it accumulated in cell bodies after just 1 hour (Fig. 3A, Fig. 4A). ProNGF uptake in DIV 7-10 BFCNs was also extremely robust, as just 50pM proNGF was enough to yield a proNGF-QD signal along the entire length of the BFCN axons (Fig. 3A, Fig 4C). For comparison, BDNF uptake was undetectable at 50pM (data not shown), and transport required at least 1nM BDNF and starvation of both axons and cell bodies (Fig. 3C-D).

Next, we assessed the effect of *in vitro* aging on proNGF uptake. Experiments were completed at DIV7-10 and DIV18-20, with the only difference being the starvation conditions required for proNGF uptake as described above; cell bodies were starved of neurotrophins and QD-proNGF was added immediately to the axonal compartment. ProNGF accumulation in DIV18-20 BFCN cell bodies was significantly diminished compared to DIV 7-10 BFCNs (Fig. 4A, B, Fig. 5, N= 100 cell bodies, $p< 0.001$, Student's *t*-test).

3.3 *Aged BFCNs Stain Positive for SaβG*

To determine if neurons cultured for extended periods of time displayed signs of aging, we carried out histological staining for SaβG. BFCNs cultured for 10 days *in vitro* did not stain for SaβG (Fig. 6A). Only BFCNs cultured for 18 days or more stained positive for SaβG (Fig. 6B, C). Staining became more pronounced as the neurons were kept longer in culture, with DIV21-24 BFCNs demonstrating robust SaβG staining (Fig. 6C). Cortical neurons did not stain positive for SaβG even at DIV24 (Fig. 6D, E).

3.4 *TrkB Immunoreactivity is Decreased in BFCNs but not Cortical Neurons Aged In Vitro*

To determine if a reduction in the BDNF receptor TrkB was facilitating the impaired BDNF transport in aged BFCNs, immunostaining for TrkB was carried out at both timepoints. DIV18 BFCNs displayed significantly reduced TrkB immunoreactivity compared to DIV10 (Fig. 7A-B, E, N= 60 cell bodies, $p<0.001$, 1-way ANOVA and *post hoc* Tukey test). TrkB immunoreactivity in cortical neurons did not change significantly with *in vitro* age (Fig. 7C-E, N= 60 cell bodies, $p=0.8$, 1-way ANOVA and *post hoc* Tukey test). TrkB immunoreactivity in DIV10 BFCNs was significantly higher compared to cortical neurons at both DIV10 and DIV18 (Fig. 7A, C-E) N= 60 cell bodies, $p<0.001$, 1-way ANOVA and *post hoc* Tukey test).

3.5 *TrkA, but not $p75^{NTR}$Immunoreactivity is Decreased in BFCNs Aged In Vitro*

To determine if a reduction in proNGF receptors TrkA and $p75^{NTR}$ was mediating the reduced proNGF uptake in DIV18-20 BFCNs, immunostaining for TrkA and $p75^{NTR}$ was carried out at both timepoints. TrkA immunoreactivity was significantly reduced in BFCNs at DIV18 compared to DIV10 (Fig. 8 N= 60 cell bodies, $p< 0.001$, Student's t-test) while $p75^{NTR}$ immunoreactivity did not change significantly between the 2 timepoints (Fig. 9 N= 60 cell bodies, $p=0.09$, Student's t-test).

4. **Discussion**

Here we characterized neurotrophin axonal transport and neurotrophin receptor expression in BFCNs. We demonstrated that both BDNF and proNGF transport diminishes with *in vitro* aging in BFCNs and that BDNF transport deficits are unique to BFCNs. For BDNF, significant increases in pause duration and decreases in axonal transport speed were seen in DIV18-20 BFCNs, but not in younger BFCNs or in DIV 18-20 cortical neurons. Cortical neurons whose axons were clearly degenerated (e.g. whose axons were no longer smooth and continuous) ceased to take up BDNF only at DIV28. For proNGF, levels of uptake were significantly diminished in DIV20 BFCNs compared to DIV8 BFCNs. BFCNs cultured for 18 days or more, but not cortical neurons, stained positive for SaβG and were the only neurons that displayed neurotrophic transport deficits. BFCNs aged *in vitro* displayed significantly reduced TrkA and TrkB immunoreactivity. $p75^{NTR}$ immunoreactivity did not change significantly in BFCNs aged *in vitro*. These findings strongly suggest that BFCNs are particularly susceptible to senescence and age-induced neurotrophin transport deficits and to TrkA and TrkB receptor downregulation.

BFCNs were much more efficient in their uptake of BDNF compared to their cortical counterparts. We found that cortical neurons required a four-hour incubation with QD-BDNF in order for transport within the microgrooves to be observed, in line with previously reported findings in hippocampal neurons (Poon et al., 2011; Zhao et al., 2014). BFCNs, on the other hand, required only one hour of incubation time. ~~perhaps due to differences in TrkB receptor levels at the axon and/or endocytic processes that allow for the rapid internalization of the TrkB-BDNF complex~~. This is most likely due to the greater TrkB expression observed in BFCNs compared to cortical neurons. BDNF uptake was slower in DIV18 BFCNs (data not shown) compared to DIV10, further implicating TrkB levels in BDNF uptake latency. Once taken up, transport speed (1μM/s) and mean pause duration (12.4s) of BDNF by DIV10 BFCNs were similar to both cortical and hippocampal neurons (Poon et al., 2011; Zhao et al., 2014). Reduced TrkB receptor levels do not account for the decreased motility of BDNF particles in DIV18

BFCNs because DIV18 cortical neurons displayed significantly less TrkB immunoreactivity compared to DIV10 BFCNs, but their BDNF transport dynamics did not differ. While differences in TrkB expression may explain the variance in BDNF uptake efficiency between cell types, the mechanism of decreased BDNF motility along axons with increased *in vitro* age remains unknown.

The efficiency of BFCN neurotrophin transport was even more evident with proNGF than with BDNF, with proNGF uptake beginning within 10 minutes of neurotrophin addition to BFCN axon terminals. This time course was even faster than in DRGs, a class of neurons in which proNGF transport is well characterized. In DRGs, proNGF transport occurs after 35 minutes (De Nadai et al., 2016; Villarin et al., 2016). Taken together, these results suggest that both CNS and PNS neurons are capable of rapid proNGF uptake and subsequent retrograde axonal transport. The functional implications of this rapid uptake are currently unknown.

The conditions required for uptake differed between BDNF and proNGF. For BDNF, both axons and cell bodies were deprived of neurotrophin for at least 1 hour before uptake was observed. For proNGF, depriving both the axons and cell bodies of neurotrophin completely inhibited uptake. This finding suggests that TrkA trafficking in BFCNs is similar to DRGs, where NGF-bound TrkA promotes the recruitment of additional TrkA receptors to axon terminals in a positive feedback loop (Yamashita et al., 2017). Cutting off neurotrophin supply to the axons abolishes this positive feedback loop, reducing TrkA trafficking to the terminals. This finding also suggests that TrkA and TrkB trafficking are governed by distinct mechanisms in BFCNs, because axonal neurotrophin starvation abolishes TrkA-mediated (proNGF) transport but not TrkB-mediated (BDNF) transport (Zhao et al., 2014).

The uptake of proNGF was diminished in BFCNs aged *in vitro*. This diminished uptake coincided with a significant decrease in TrkA receptor immunoreactivity. $P75^{NTR}$ immunoreactivity did not decrease with *in vitro* age. These findings suggest that the reduction of TrkA receptor levels is responsible for the reduced uptake of proNGF by BFCNs aged *in vitro*. $p75^{NTR}$ has a higher binding affinity for proNGF

compared to TrkA (Clewes et al., 2008; Nykjaer et al., 2004). However, its maintenance in DIV18 BFCNs did not result in maintenance of proNGF transport at this timepoint, suggesting that the balance between TrkA and $p75^{NTR}$ levels is important for the retrograde transport of proNGF and that loss of TrkA contributes to reduced proNGF transport in aged BFCNs.

Although the uptake of proNGF was diminished in aged BFCNs, the robust level of uptake observed in young BFCNs was surprising. 50pM of proNGF was enough to observe a proNGF-QD signal along the entire length of the microgrooves. This rapid and robust uptake of proNGF made generating kymographs with individual trackable particles difficult. With BDNF, even concentrations of over 1nM resulted in few particles populating the microgrooves. These results strongly suggest that proNGF uptake is more efficient than BDNF uptake in BFCNs.

One of the key limitations of this work is the *in vitro* model of aging. Cultured CNS neurons are viable for 3-4 weeks in culture before they degenerate. With the lifespan of healthy rats being around 2 years, the degeneration seen *in vitro* occurs at an accelerated rate compared to *in vivo*. However, many of the hallmarks associated with neuronal aging *in vivo* are recapitulated *in vitro*. Hippocampal neurons kept in culture for 3 weeks display ROS accumulation, lipofuscin granules, loss of cholesterol from cell membranes, and activation of both the pJNK and p53/p21 pathways, all of which are also seen in neurons taken from aged animals (Brewer et al., 2007; Calvo et al., 2015; Porter et al., 1997; Sodero et al., 2011). Furthermore, it has recently been demonstrated that general axonal transport through the septohippocampal tract is reduced *in vivo* with normal aging in mice and is exacerbated by AD pathology (Bearer et al., 2018). Our BFCNs, but not cortical neurons, stained positive for SaβG at DIV18, a well validated marker of aging both *in vivo* and *in vitro.* By DIV28, axons were clearly degenerating in both groups. TrkA downregulation in the absence of $p75^{NTR}$ downregulation has been repeatedly observed in both aging and AD-affected basal forebrain neurons in humans and rodents (Fahnestock and Shekari, 2019; Gibbs, 1998; Ginsberg et al., 2006; Mufson et al., 2000; Niewiadomska et al., 2002). Thus, while the molecular mechanisms underlying neuronal degeneration *in vivo* are accelerated *in vitro*, they are not

dissimilar. Studying *in vitro* aging provides an effective way to gain insight into the mechanisms underlying aging in paradigms where *in vivo* work is difficult.

In conclusion, our data suggest that BFCNs display unique, age-dependent deficits in TrkA and TrkB receptor expression and the retrograde axonal transport of BDNF and proNGF. These deficits support previous findings that demonstrate the susceptibility of the basal forebrain to age-related degeneration and may explain the extreme susceptibility of the basal forebrain to AD. The basal forebrain projects to almost all areas of the cortex and the hippocampus. It plays canonical and crucial roles in learning, memory and attention and is also involved in other important functions including regulation of blood flow to the cortex. Understanding how and why these neurons degenerate both with age and in AD is critical for our understanding of aging, neurodegenerative diseases and the nervous system as a whole.

Figure Legends.

Fig 1. BDNF Transport in Basal Forebrain and Cortical Neurons Aged in Culture. Kymographs of quantum-dot labelled BDNF (QD-BDNF) particles within the microgrooves of basal forebrain cholinergic neurons (BFCN, A-F) and cortical neurons (CTX, G-I) in microfluidic chambers. Horizontal/diagonal lines represent movement in the anterograde or retrograde direction as indicated by open or closed arrows, respectively. Vertical line segments indicate instances of no movement or pausing. Neurons were cultured for at least 7 days *in* vitro (DIV) to allow axons to fully traverse the microgrooves. Images were taken 1 hour after 1nM QD-BDNF was added to the axon terminal side only. Aged (DIV21) BFCNs clearly show stationary BDNF-QD (D-F).

Fig 2. BDNF Transport Speed and Pause Duration in Basal Forebrain and Cortical Neurons Aged in Culture. Quantification of speed (A) and pause duration (B) of quantum-dot labelled BDNF (QD-BDNF) in basal forebrain cholinergic neurons (BFCN) and cortical neurons (CTX). Data were collected 1 hour after 1nM QD-BDNF was added to the axon terminal side of the microfluidic chambers for BFCNs, and 4 hours for cortical neurons. Neurons cultured for either 7-10 days *in vitro* (DIV) or 18-20 DIV. The mTrackJ plug-in for ImageJ was used to determine the distanced travelled by QD-BDNF particles between time-lapse images. Each bar shows N= 60 QD-BDNF particles from 3 different chambers and 3 rounds of dissection (5 embryos each). Data represented as means $\pm$SE. **p<0.01, ***p<0.001, 1-way ANOVA and *post-hoc* Tukey test.

Figure 3. Representative Uptake of Neurotrophins in Basal Forebrain Neurons. proNGF uptake **(C)** by BFCNs is more robust than BDNF uptake **(A, B)**. proNGF uptake conditions differ from BDNF **(A-D)**. All images were taken at the first instance of fluorescence in the microgrooves following QD-labelled neurotrophin administration to axon terminals only. For QD-BDNF, images were taken 1 hour following neurotrophin starvation of axons and cell bodies overnight. For QD-proNGF, images were taken 15

minutes following immediate neurotrophin starvation of cell bodies only. Individual microgrooves visualized.

Fig 4. Uptake and Transport of Quantum-Dot Labelled proNGF (QD-proNGF) in Basal Forebrain Cholinergic Neurons (BFCNs). Data were collected 1 hour after 50pM QD-proNGF[R-1G] was added to the axon terminal side of the microfluidic chambers. **A and B:** Cell bodies; **C and D:** microgrooves (axons).

Fig 5. Quantification of Quantum-Dot Labelled proNGF (QD-proNGF) Uptake by Basal Forebrain Cholinergic Neurons (BFCNs). BFCN cell bodies demonstrated more proNGF[R-1G] at DIV8 compared to DIV20. *N*= 100 cell bodies per group, from 3 different chambers and 2 rounds of dissection (5 embryos each). Data represented as mean $\pm$SE. ***$p<0.001$ by Student's *t*-test.

Fig 6. Senescence-Associated Beta Galactosidase Stain of Basal Forebrain and Cortical Neurons Aged in Culture. DIV10 basal forebrain (BFCN) and cortical (CTX) neurons do not stain for senescence-associated beta-galactosidase. BFCNs begin to stain positive at DIV18, with more pronounced staining occurring at DIV24. DIV24 CTX neurons do not stain positive for senescence-associated beta-galactosidase. Arrows indicate labelled cell bodies.

Fig 7. Decreased TrkB Immunoreactivity in Basal Forebrain Cholinergic Neurons (BFCNs) but not Cortical Neurons (CTX) aged *In Vitro*. BFCN cell bodies demonstrated significantly less TrkB immunoreactivity at DIV18 compared to DIV10. TrkB immunoreactivity did not change significantly in cortical neurons between DIV10 and DIV18. TrkB immunoreactivity was significantly greater in BFCNs at DIV10 compared to CTX at all time points. Each bar shows *N*= 60 cell bodies from 3 different chambers and 3 rounds of dissection (5 embryos each). Data represented as means $\pm$SE. ***$p<0.001$, "ns" = not significant ($p=0.8$) 1-way ANOVA and *post-hoc* Tukey test.

Fig 8. Decreased TrkA Immunoreactivity in Basal Forebrain Cholinergic Neurons (BFCNs) Aged *In Vitro*. BFCN cell bodies demonstrated significantly less TrkA immunoreactivity at DIV18 compared

to DIV10. N= 60 cell bodies per group, from 3 different chambers and 3 rounds of dissection (5 embryos each). Data represented as mean +SE. ***p<0.001 by Student's t-test.

Fig. 9. $p75^{NTR}$ Immunoreactivity in Basal Forebrain Cholinergic Neurons (BFCNs) Does Not Change During Aging *In Vitro*. $p75^{NTR}$ immunoreactivity did not change significantly between DIV10 and DIV18 in BFCNs. N= 60 cell bodies per group, from 3 different chambers and 3 rounds of dissection (5 embryos each). Data represented as mean +SE. p=0.09 by Student's t-test. "ns" = not significant (p=0.8)

Supplementary Figure 1. TrkA and VAChT Staining in BFCNs. Basal forebrain neurons grown in microfluidic chambers for 10 days stained with an antibody against TrkA (A) and vesicular acetylcholine transporter (B). Cortical neurons did not stain with either marker (C).

Supplementary Figure 2. Western blot of proNGF purified from HEK cell medium. Blots were completed as described in Fahnestock et al. (2001). 50 pg of nickel-affinity purified protein loaded in lane 1, 100 pg recombinant mature NGF (a generous gift from Dr. Michael Coughlin, McMaster University) loaded in lane 2, and elution buffer (no recombinant protein) loaded in lane 3. No mature NGF was detected in the purified protein sample.

References

Altavista, M.C., Rossi, P., Bentivoglio, A.R., Crociani, P., Albanese, A., 1990. Aging is associated with a diffuse impairment of forebrain cholinergic neurons. Brain Res. https://doi.org/10.1016/0006-8993(90)91116-X

Baker-Nigh, A., Vahedi, S., Davis, E.G., Weintraub, S., Bigio, E.H., Klein, W.L., Geula, C., 2015. Neuronal amyloid-β accumulation within cholinergic basal forebrain in ageing and Alzheimer's disease. Brain 138, 1722–1737. https://doi.org/10.1093/brain/awv024

Ballinger, E.C., Ananth, M., Talmage, D.A., Role, L.W., 2016. Basal Forebrain Cholinergic Circuits and Signaling in Cognition and Cognitive Decline. Neuron. https://doi.org/10.1016/j.neuron.2016.09.006

Baxter, M.G., Chiba, A.A., 1999. Cognitive functions of the basal forebrain. Curr. Opin. Neurobiol. 9, 178–183. https://doi.org/10.1016/S0959-4388(99)80024-5

Bearer, E.L., Manifold-Wheeler, B.C., Medina, C.S., Gonzales, A.G., Chaves, F.L., Jacobs, R.E., 2018. Alterations of functional circuitry in aging brain and the impact of mutated APP expression. Neurobiol. Aging. https://doi.org/10.1016/j.neurobiolaging.2018.06.018

Bothwell, M., 2014. NGF, BDNF, NT3, and NT4. Handb. Exp. Pharmacol. https://doi.org/10.1007/978-3-642-45106-5_1

Brewer, L.D., Thibault, O., Staton, J., Thibault, V., Rogers, J.T., Garcia-Ramos, G., Kraner, S., Landfield, P.W., Porter, N.M., 2007. Increased vulnerability of hippocampal neurons with age in culture: Temporal association with increases in NMDA receptor current, NR2A subunit expression and recruitment of L-type calcium channels. Brain Res. https://doi.org/10.1016/j.brainres.2007.03.020

Calvo, M., Sanz-Blasco, S., Caballero, E., Villalobos, C., Núñez, L., 2015. Susceptibility to excitotoxicity in aged hippocampal cultures and neuroprotection by non-steroidal anti-inflammatory drugs: Role of mitochondrial calcium. J. Neurochem. https://doi.org/10.1111/jnc.13004

Campos, P.B., Paulsen, B.S., Rehen, S.K., 2014. Accelerating neuronal aging in in vitro model brain disorders: A focus on reactive oxygen species. Front. Aging Neurosci. https://doi.org/10.3389/fnagi.2014.00292

Clewes, O., Fahey, M.S., Tyler, S.J., Watson, J.J., Seok, H., Catania, C., Cho, K., Dawbarn, D., Allen, S.J., 2008. Human ProNGF: Biological effects and binding profiles at TrkA, P75NTRand sortilin. J. Neurochem. 107, 1124–1135. https://doi.org/10.1111/j.1471-4159.2008.05698.x

Cooper, J.D., Lindholm, D., Sofroniew, M. V., 1994. Reduced transport of [125I]nerve growth factor by cholinergic neurons and down-regulated trka expression in the medial septum of aged rats. Neuroscience. https://doi.org/10.1016/0306-4522(94)90462-6

Cooper, J.D., Salehi, A., Delcroix, J.-D., Howe, C.L., Belichenko, P. V, Chua-Couzens, J., Kilbridge, J.F., Carlson, E.J., Epstein, C.J., Mobley, W.C., 2001. Failed retrograde transport of NGF in a mouse model of Down's syndrome: Reversal of cholinergic neurodegenerative phenotypes following NGF infusion. Proc. Natl. Acad. Sci. https://doi.org/10.1073/pnas.181219298

Counts, S.E., Nadeem, M., Wuu, J., Ginsberg, S.D., Saragovi, H.U., Mufson, E.J., 2004. Reduction of cortical TrkA but not p75 NTR protein in early-stage Alzheimer's disease. Ann. Neurol. 56, 520–531. https://doi.org/10.1002/ana.20233

De Lacalle, S., Cooper, J.D., Svendsen, C.N., Dunnett, S.B., Sofroniew, M. V., 1996. Reduced retrograde labelling with fluorescent tracer accompanies neuronal atrophy of basal forebrain cholinergic neurons in aged rats. Neuroscience. https://doi.org/10.1016/0306-4522(96)00239-4

De Nadai, T., Marchetti, L., Di Rienzo, C., Calvello, M., Signore, G., Di Matteo, P., Gobbo, F., Turturro, S., Meucci, S., Viegi, A., Beltram, F., Luin, S., Cattaneo, A., 2016. Precursor and mature NGF live tracking: One versus many at a time in the axons. Sci. Rep. 6. https://doi.org/10.1038/srep20272

Dimri, G.P., Lee, X., Basile, G., Acosta, M., Scott, G., Roskelley, C., Medrano, E.E., Linskens, M.,

Rubelj, I., Pereira-Smith, O., 1995. A biomarker that identifies senescent human cells in culture and in aging skin in vivo. Proc. Natl. Acad. Sci. U. S. A. https://doi.org/DOI 10.1073/pnas.92.20.9363

DiStefano, P.S., Friedman, B., Radziejewski, C., Alexander, C., Boland, P., Schick, C.M., Lindsay, R.M., Wiegand, S.J., 1992. The neurotrophins BDNF, NT-3, and NGF display distinct patterns of retrograde axonal transport in peripheral and central neurons. Neuron 8, 983–993. https://doi.org/10.1016/0896-6273(92)90213-W

Fahnestock, M., Michalski, B., Xu, B., Coughlin, M.D., 2001. The precursor pro-nerve growth factor is the predominant form of nerve growth factor in brain and is increased in Alzheimer's disease. Mol. Cell. Neurosci. 18, 210–220. https://doi.org/10.1006/mcne.2001.1016

Fahnestock, M., Shekari, A., 2019. ProNGF and Neurodegeneration in Alzheimer's Disease. Front. Neurosci. 13. https://doi.org/10.3389/fnins.2019.00129

Fahnestock, M., Yu, G., Michalski, B., Mathew, S., Colquhoun, A., Ross, G.M., Coughlin, M.D., 2004. The nerve growth factor precursor proNGF exhibits neurotrophic activity but is less active than mature nerve growth factor. J. Neurochem. 89, 581–592. https://doi.org/10.1111/j.1471-4159.2004.02360.x

Fragkouli, A., Hearn, C., Errington, M., Cooke, S., Grigoriou, M., Bliss, T., Stylianopoulou, F., Pachnis, V., 2005. Loss of forebrain cholinergic neurons and impairment in spatial learning and memory in LHX7-deficient mice. Eur. J. Neurosci. https://doi.org/10.1111/j.1460-9568.2005.04141.x

Gibbs, R.B., 1998. Impairment of basal forebrain cholinergic neurons associated with aging and long-term loss of ovarian function. Exp. Neurol. 151, 289–302. https://doi.org/10.1006/exnr.1998.6789

Ginsberg, S.D., Che, S., Wuu, J., Counts, S.E., Mufson, E.J., 2006. Down regulation of trk but not p75NTR gene expression in single cholinergic basal forebrain neurons mark the progression of Alzheimer's disease. J. Neurochem. https://doi.org/10.1111/j.1471-4159.2006.03764.x

Götz, J., Chen, F., van Dorpe, J., Nitsch, R.M., 2001. Formation of neurofibrillary tangles in P301l tau transgenic mice induced by Abeta 42 fibrils. Science 293, 1491–5. https://doi.org/10.1126/science.1062097

Grothe, M., Heinsen, H., Teipel, S.J., 2012. Atrophy of the cholinergic basal forebrain over the adult age range and in early stages of Alzheimer's disease. Biol. Psychiatry. https://doi.org/10.1016/j.biopsych.2011.06.019

Gustilo, M.C., Markowska, A.L., Breckler, S.J., Fleischman, C.A., Price, D.L., Koliatsos, V.E., 1999. Evidence that nerve growth factor influences recent memory through structural changes in septohippocampal cholinergic neurons. J. Comp. Neurol. https://doi.org/10.1002/(SICI)1096-9861(19990322)405:4<491::AID-CNE4>3.0.CO;2-N

H. Ferreira-Vieira, T., M. Guimaraes, I., R. Silva, F., M. Ribeiro, F., 2016. Alzheimer's disease: Targeting the Cholinergic System. Curr. Neuropharmacol. https://doi.org/10.2174/1570159X13666150716165726

Ioannou, M.S., Fahnestock, M., 2017. ProNGF, but not NGF, switches from neurotrophic to apoptotic activity in response to reductions in TrKA receptor levels. Int. J. Mol. Sci. 18. https://doi.org/10.3390/ijms18030599

Kurz, D.J., Decary, S., Hong, Y., Erusalimsky, J.D., 2000. Senescence-associated (beta)-galactosidase reflects an increase in lysosomal mass during replicative ageing of human endothelial cells. J. Cell Sci.

Linville, D.G., Arnerić, S.P., 1991. Cortical cerebral blood flow governed by the basal forebrain: Age-related Impairments. Neurobiol. Aging. https://doi.org/10.1016/0197-4580(91)90080-4

Martin, M.G., Perga, S., Trovo, L., Rasola, A., Holm, P., Rantamaki, T., Harkany, T., Castren, E., Chiara, F., Dotti, C.G., 2008. Cholesterol Loss Enhances TrkB Signaling in Hippocampal Neurons Aging in

Vitro. Mol. Biol. Cell. https://doi.org/10.1091/mbc.E07-09-0897

Masoudi, R., Ioannou, M.S., Coughlin, M.D., Pagadala, P., Neet, K.E., Clewes, O., Allen, S.J., Dawbarn, D., Fahnestock, M., 2009. Biological activity of nerve growth factor precursor is dependent upon relative levels of its receptors. J. Biol. Chem. https://doi.org/10.1074/jbc.M109.007104

Mishima, K., Handa, J.T., Aotaki-Keen, A., Lutty, G.A., Morse, L.S., Hjelmeland, L.M., 1999. Senescence-associated β-galactosidase histochemistry for the primate eye. Investig. Ophthalmol. Vis. Sci.

Mufson, E.J., Ginsberg, S.D., Ikonomovic, M.D., DeKosky, S.T., 2003. Human cholinergic basal forebrain: Chemoanatomy and neurologic dysfunction, in: Journal of Chemical Neuroanatomy. https://doi.org/10.1016/S0891-0618(03)00068-1

Mufson, E.J., Ma, S.Y., Cochran, E.J., Bennett, D.A., Beckett, L.A., Jaffar, S., Saragovi, H.U., Kordower, J.H., 2000. Loss of nucleus basalis neurons containing trkA immunoreactivity in individuals with mild cognitive impairment and early Alzheimer's diseases. J. Comp. Neurol. https://doi.org/10.1002/1096-9861(20001106)427:1<19::AID-CNE2>3.0.CO;2-A

Niewiadomska, G., Komorowski, S., Baksalerska-Pazera, M., 2002. Amelioration of cholinergic neurons dysfunction in aged rats depends on the continuous supply of NGF. Neurobiol. Aging. https://doi.org/10.1016/S0197-4580(01)00345-1

Nykjaer, A., Lee, R., Teng, K.K., Jansen, P., Madsen, P., Nielsen, M.S., Jacobsen, C., Kliemannel, M., Schwarz, E., Willnow, T.E., Hempstead, B.L., Petersen, C.M., 2004. Sortilin is essential for proNGF-induced neuronal cell death. Nature. https://doi.org/10.1038/nature02319

Palomer, E., Martín-Segura, A., Baliyan, S., Ahmed, T., Balschun, D., Venero, C., Martin, M.G., Dotti, C.G., 2016. Aging Triggers a Repressive Chromatin State at Bdnf Promoters in Hippocampal Neurons. Cell Rep. https://doi.org/10.1016/j.celrep.2016.08.028

Parikh, V., Howe, W.M., Welchko, R.M., Naughton, S.X., D'Amore, D.E., Han, D.H., Deo, M., Turner, D.L., Sarter, M., 2013. Diminished trkA receptor signaling reveals cholinergic-attentional vulnerability of aging. Eur. J. Neurosci. https://doi.org/10.1111/ejn.12090

Poon, W.W., Blurton-Jones, M., Tu, C.H., Feinberg, L.M., Chabrier, M.A., Harris, J.W., Jeon, N.L., Cotman, C.W., 2011. β-Amyloid impairs axonal BDNF retrograde trafficking. Neurobiol. Aging 32, 821–833. https://doi.org/10.1016/j.neurobiolaging.2009.05.012

Porter, N.M., Thibault, O., Thibault, V., Chen, K.C., Landfield, P.W., 1997. Calcium channel density and hippocampal cell death with age in long-term culture. J. Neurosci.

Salehi, A., Delcroix, J.D., Belichenko, P. V., Zhan, K., Wu, C., Valletta, J.S., Takimoto-Kimura, R., Kleschevnikov, A.M., Sambamurti, K., Chung, P.P., Xia, W., Villar, A., Campbell, W.A., Kulnane, L.S., Nixon, R.A., Lamb, B.T., Epstein, C.J., Stokin, G.B., Goldstein, L.S.B., Mobley, W.C., 2006. Increased App Expression in a Mouse Model of Down's Syndrome Disrupts NGF Transport and Causes Cholinergic Neuron Degeneration. Neuron. https://doi.org/10.1016/j.neuron.2006.05.022

Schmitz, T.W., Nathan Spreng, R., Weiner, M.W., Aisen, P., Petersen, R., Jack, C.R., Jagust, W., Trojanowki, J.Q., Toga, A.W., Beckett, L., Green, R.C., Saykin, A.J., Morris, J., Shaw, L.M., Khachaturian, Z., Sorensen, G., Kuller, L., Raichle, M., Paul, S., Davies, P., Fillit, H., Hefti, F., Holtzman, D., Mesulam, M.M., Potter, W., Snyder, P., Schwartz, A., Montine, T., Thomas, R.G., Donohue, M., Walter, S., Gessert, D., Sather, T., Jiminez, G., Harvey, D., Bernstein, M., Fox, N., Thompson, P., Schuff, N., Borowski, B., Gunter, J., Senjem, M., Vemuri, P., Jones, D., Kantarci, K., Ward, C., Koeppe, R.A., Foster, N., Reiman, E.M., Chen, K., Mathis, C., Landau, S., Cairns, N.J., Householder, E., Taylor-Reinwald, L., Lee, V., Korecka, M., Figurski, M., Crawford, K., Neu, S., Foroud, T.M., Potkin, S., Shen, L., Faber, K., Kim, S., Nho, K., Thal, L., Buckholtz, N., Albert, Marylyn, Frank, R., Hsiao, J., Kaye, J., Quinn, J., Lind, B., Carter, R., Dolen, S., Schneider, L.S., Pawluczyk, S., Beccera, M., Teodoro, L., Spann, B.M., Brewer, J., Vanderswag, H., Fleisher, A.,

Heidebrink, J.L., Lord, J.L., Mason, S.S., Albers, C.S., Knopman, D., Johnson, Kris, Doody, R.S., Villanueva-Meyer, J., Chowdhury, M., Rountree, S., Dang, M., Stern, Y., Honig, L.S., Bell, K.L., Ances, B., Carroll, M., Leon, S., Mintun, M.A., Schneider, S., Oliver, A., Marson, D., Griffith, R., Clark, D., Geldmacher, D., Brockington, J., Roberson, E., Grossman, H., Mitsis, E., de Toledo-Morrell, L., Shah, R.C., Duara, R., Varon, D., Greig, M.T., Roberts, P., Albert, Marilyn, Onyike, C., D'Agostino, D., Kielb, S., Galvin, J.E., Cerbone, B., Michel, C.A., Rusinek, H., de Leon, M.J., Glodzik, L., De Santi, S., Doraiswamy, P.M., Petrella, J.R., Wong, T.Z., Arnold, S.E., Karlawish, J.H., Wolk, D., Smith, C.D., Jicha, G., Hardy, P., Sinha, P., Oates, E., Conrad, G., Lopez, O.L., Oakley, M., Simpson, D.M., Porsteinsson, A.P., Goldstein, B.S., Martin, K., Makino, K.M., Ismail, M.S., Brand, C., Mulnard, R.A., Thai, G., Mc-Adams-Ortiz, C., Womack, K., Mathews, D., Quiceno, M., Diaz-Arrastia, R., King, R., Weiner, M., Martin-Cook, K., DeVous, M., Levey, A.I., Lah, J.J., Cellar, J.S., Burns, J.M., Anderson, H.S., Swerdlow, R.H., Apostolova, L., Tingus, K., Woo, E., Silverman, D.H.S., Lu, P.H., Bartzokis, G., Graff-Radford, N.R., Parfitt, F., Kendall, T., Johnson, H., Farlow, M.R., Hake, A., Matthews, B.R., Herring, S., Hunt, C., van Dyck, C.H., Carson, R.E., MacAvoy, M.G., Chertkow, H., Bergman, H., Hosein, C., Black, S., Stefanovic, B., Caldwell, C., Robin Hsiung, G.-Y., Feldman, H., Mudge, B., Assaly, M., Kertesz, A., Rogers, J., Bernick, C., Munic, D., Kerwin, D., Mesulam, M.-M., Lipowski, K., Wu, C.-K., Johnson, N., Sadowsky, C., Martinez, W., Villena, T., Turner, R.S., Johnson, Kathleen, Reynolds, B., Sperling, R.A., Johnson, K.A., Marshall, G., Frey, M., Lane, B., Rosen, A., Tinklenberg, J., Sabbagh, M.N., Belden, C.M., Jacobson, S.A., Sirrel, S.A., Kowall, N., Killiany, R., Budson, A.E., Norbash, A., Johnson, P.L., Allard, J., Lerner, A., Ogrocki, P., Hudson, L., Fletcher, E., Carmichael, O., Olichney, J., DeCarli, C., Kittur, S., Borrie, M., Lee, T.-Y., Bartha, R., Johnson, S., Asthana, S., Carlsson, C.M., Potkin, S.G., Preda, A., Nguyen, D., Tariot, P., Reeder, S., Bates, V., Capote, H., Rainka, M., Scharre, D.W., Kataki, M., Adeli, A., Zimmerman, E.A., Celmins, D., Brown, A.D., Pearlson, G.D., Blank, K., Anderson, K., Santulli, R.B., Kitzmiller, T.J., Schwartz, E.S., Sink, K.M., Williamson, J.D., Garg, P., Watkins, F., Ott, B.R., Querfurth, H., Tremont, G., Salloway, S., Malloy,

P., Correia, S., Rosen, H.J., Miller, B.L., Mintzer, J., Spicer, K., Bachman, D., Finger, E., Pasternak, S., Rachinsky, I., Drost, D., Pomara, N., Hernando, R., Sarrael, A., Schultz, S.K., Boles Ponto, L.L., Shim, H., Smith, K.E., Relkin, N., Chaing, G., Raudin, L., Smith, A., Fargher, K., Raj, B.A., Neylan, T., Grafman, J., Davis, M., Morrison, R., Hayes, J., Finley, S., Friedl, K., Fleischman, D., Arfanakis, K., James, O., Massoglia, D., Fruehling, J.J., Harding, S., Peskind, E.R., Petrie, E.C., Li, G., Yesavage, J.A., Taylor, J.L., Furst, A.J., 2016. Basal forebrain degeneration precedes and predicts the cortical spread of Alzheimer's pathology. Nat. Commun. 7, 13249. https://doi.org/10.1038/ncomms13249

Scott, S.A., Mufson, E.J., Weingartner, J.A., Skau, K.A., Crutcher, K.A., 1995. Nerve growth factor in Alzheimer's disease: increased levels throughout the brain coupled with declines in nucleus basalis. J. Neurosci. 15, 6213–6221.

Seiler, M., Schwab, M.E., 1984. Specific retrograde transport of nerve growth factor (NGF) from neocortex to nucleus basalis in the rat. Brain Res. 300, 33–39. https://doi.org/10.1016/0006-8993(84)91338-6

Sobreviela, T., Pagcatipunan, M., Kroin, J.S., Mufson, E.J., 1996. Retrograde transport of brain-derived neurotrophic factor (BDNF) following infusion in neo- and limbic cortex in rat: Relationship to BDNF mRNA expressing neurons. J. Comp. Neurol. https://doi.org/10.1002/(SICI)1096-9861(19961118)375:3<417::AID-CNE6>3.0.CO;2-5

Sodero, A.O., Weissmann, C., Ledesma, M.D., Dotti, C.G., 2011. Cellular stress from excitatory neurotransmission contributes to cholesterol loss in hippocampal neurons aging in vitro. Neurobiol. Aging. https://doi.org/10.1016/j.neurobiolaging.2010.06.001

Sung, K., Maloney, M.T., Yang, J., Wu, C., 2011. A novel method for producing mono-biotinylated, biologically active neurotrophic factors: An essential reagent for single molecule study of axonal transport. J. Neurosci. Methods 200, 121–128. https://doi.org/10.1016/j.jneumeth.2011.06.020

Teipel, S., Heinsen, H., Amaro, E., Grinberg, L.T., Krause, B., Grothe, M., 2014. Cholinergic basal forebrain atrophy predicts amyloid burden in Alzheimer's disease. Neurobiol. Aging. https://doi.org/10.1016/j.neurobiolaging.2013.09.029

Uday Bhanu, M., Mandraju, R.K., Bhaskar, C., Kondapi, A.K., 2010. Cultured cerebellar granule neurons as an in vitro aging model: Topoisomerase IIβ as an additional biomarker in DNA repair and aging. Toxicol. Vitr. https://doi.org/10.1016/j.tiv.2010.08.003

Villarin, J.M., McCurdy, E.P., Martínez, J.C., Hengst, U., 2016. Local synthesis of dynein cofactors matches retrograde transport to acutely changing demands. Nat. Commun. 7. https://doi.org/10.1038/ncomms13865

Whitehouse, P.J., Price, D.L., Struble, R.G., Clark, A.W., Coyle, J.T., DeLong, M.R., 1982. Alzheimer's disease and senile dementia: Loss of neurons in the basal forebrain. Science (80-.). https://doi.org/10.1126/science.7058341

Williams, B., Granholm, A.C., Sambamurti, K., 2007. Age-dependent loss of NGF signaling in the rat basal forebrain is due to disrupted MAPK activation. Neurosci. Lett. https://doi.org/10.1016/j.neulet.2006.11.040

Williams, B.J., Bimonte-Nelson, H.A., Granholm-Bentley, A.C., 2006. ERK-mediated NGF signaling in the rat septo-hippocampal pathway diminishes with age. Psychopharmacology (Berl). https://doi.org/10.1007/s00213-006-0477-1

Yamashita, N., Joshi, R., Zhang, S., Zhang, Z.Y., Kuruvilla, R., 2017. Phospho-Regulation of Soma-to-Axon Transcytosis of Neurotrophin Receptors. Dev. Cell 42, 626-639.e5. https://doi.org/10.1016/j.devcel.2017.08.009

Ypsilanti, A.R., Girão da Cruz, M.T., Burgess, A., Aubert, I., 2008. The length of hippocampal cholinergic fibers is reduced in the aging brain. Neurobiol. Aging 29, 1666–1679.

https://doi.org/10.1016/j.neurobiolaging.2007.04.001

Zhao, X., Zhou, Y., Weissmiller, A.M., Pearn, M.L., Mobley, W.C., Wu, C., 2014. Real-time Imaging of Axonal Transport of Quantum Dot-labeled BDNF in Primary Neurons. J. Vis. Exp. 1–8. https://doi.org/10.3791/51899

Figure 1.

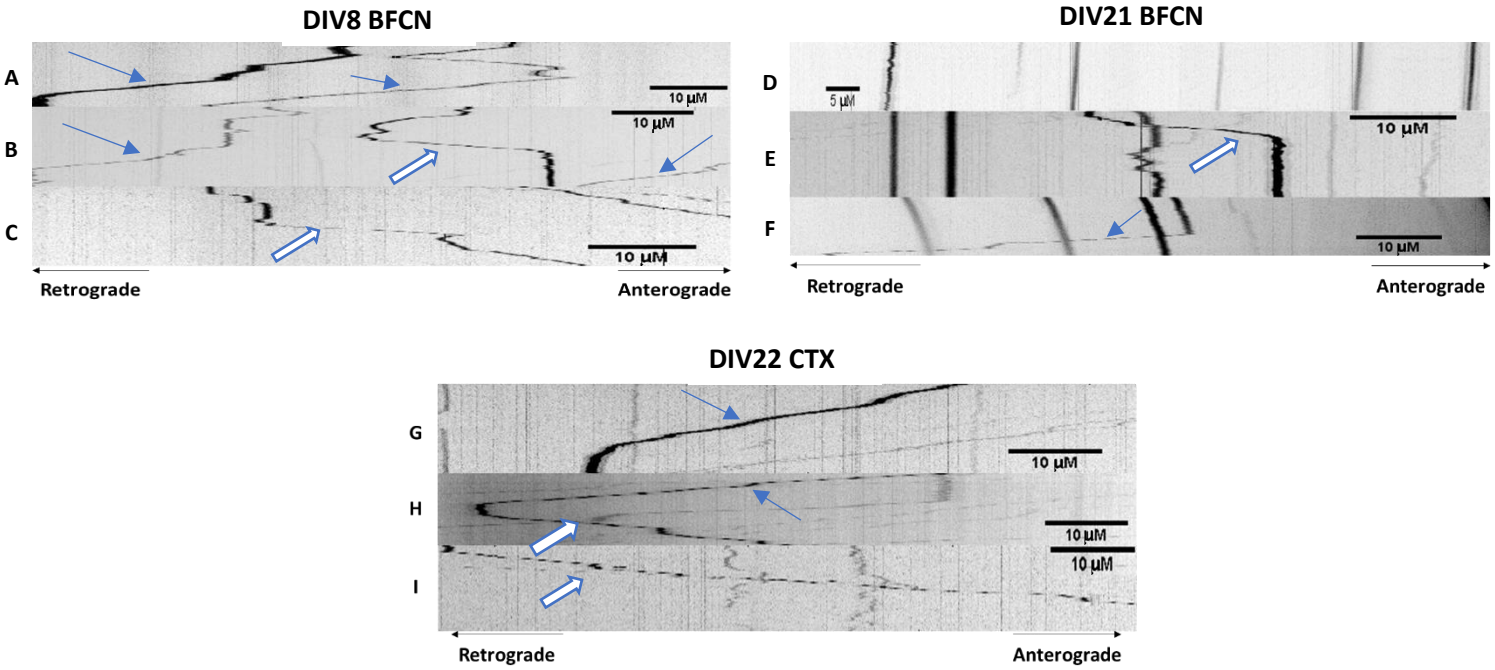

Figure 2.

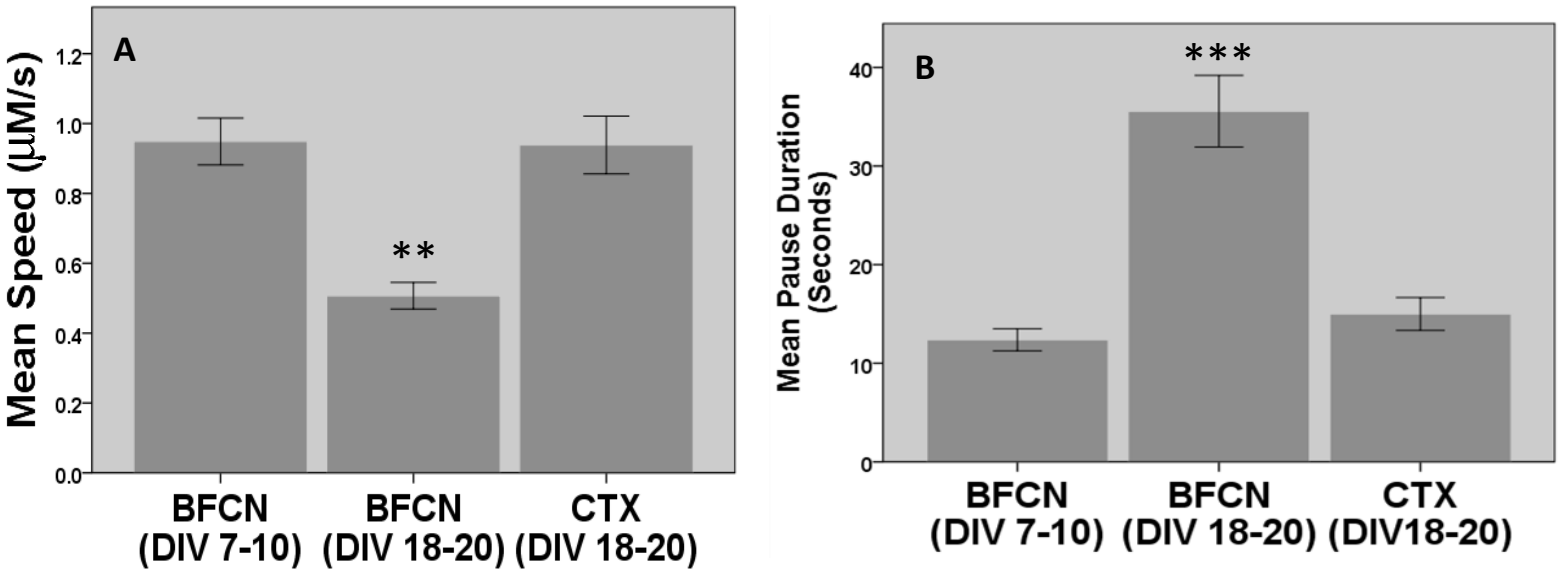

Figure 3.

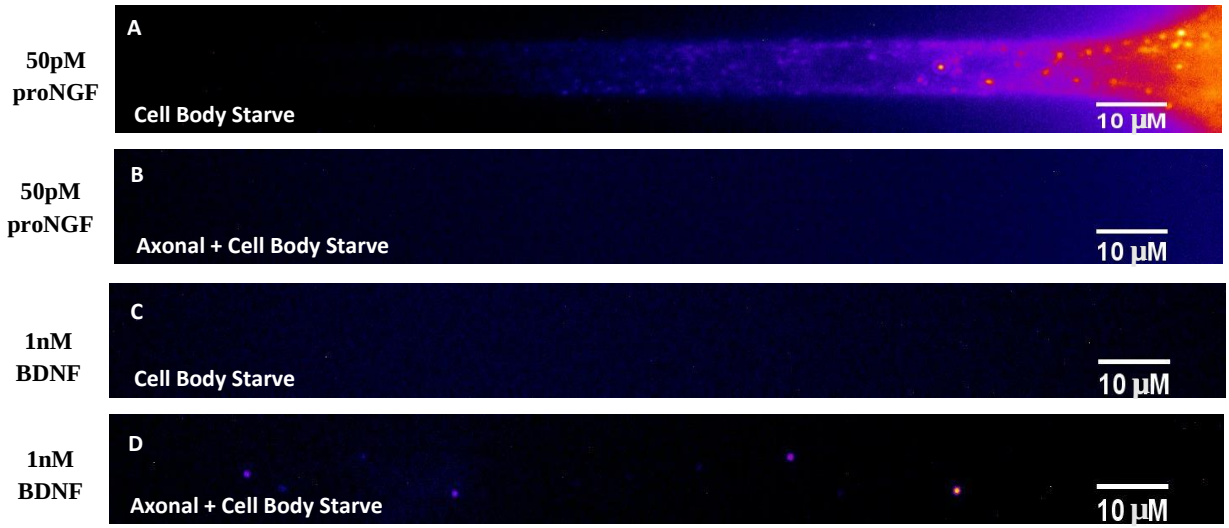

Figure 4.

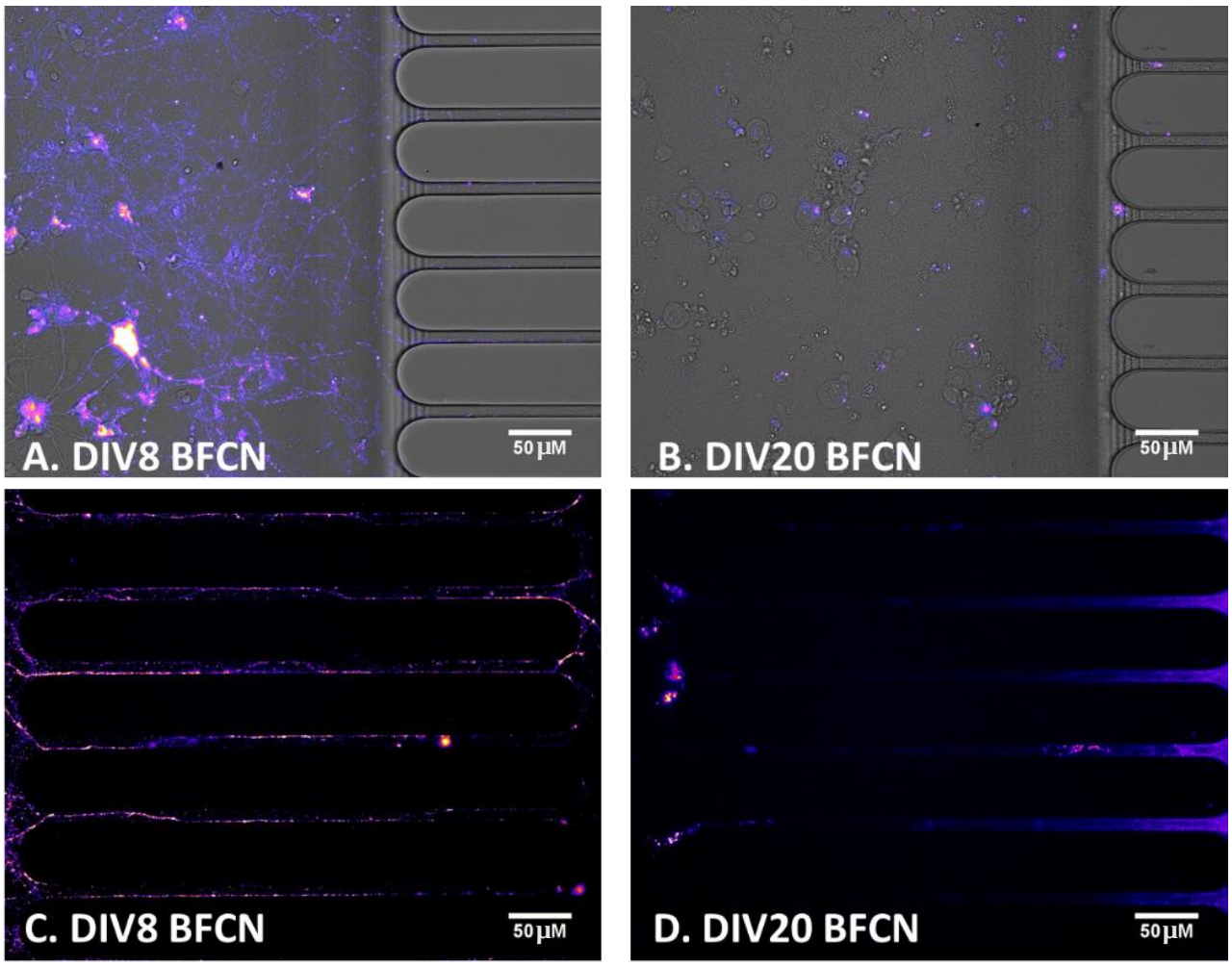

Figure 5.

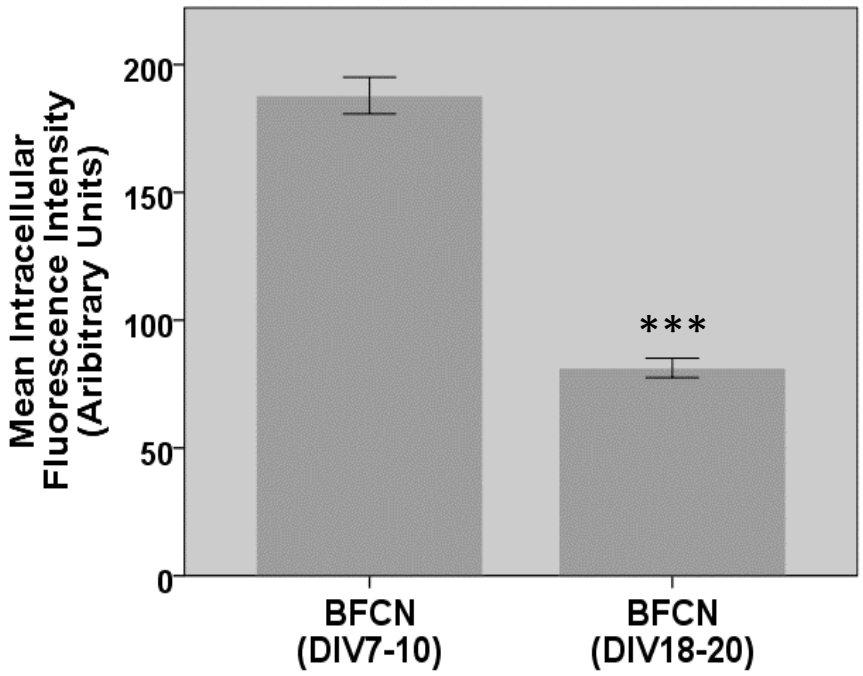

Figure 6.

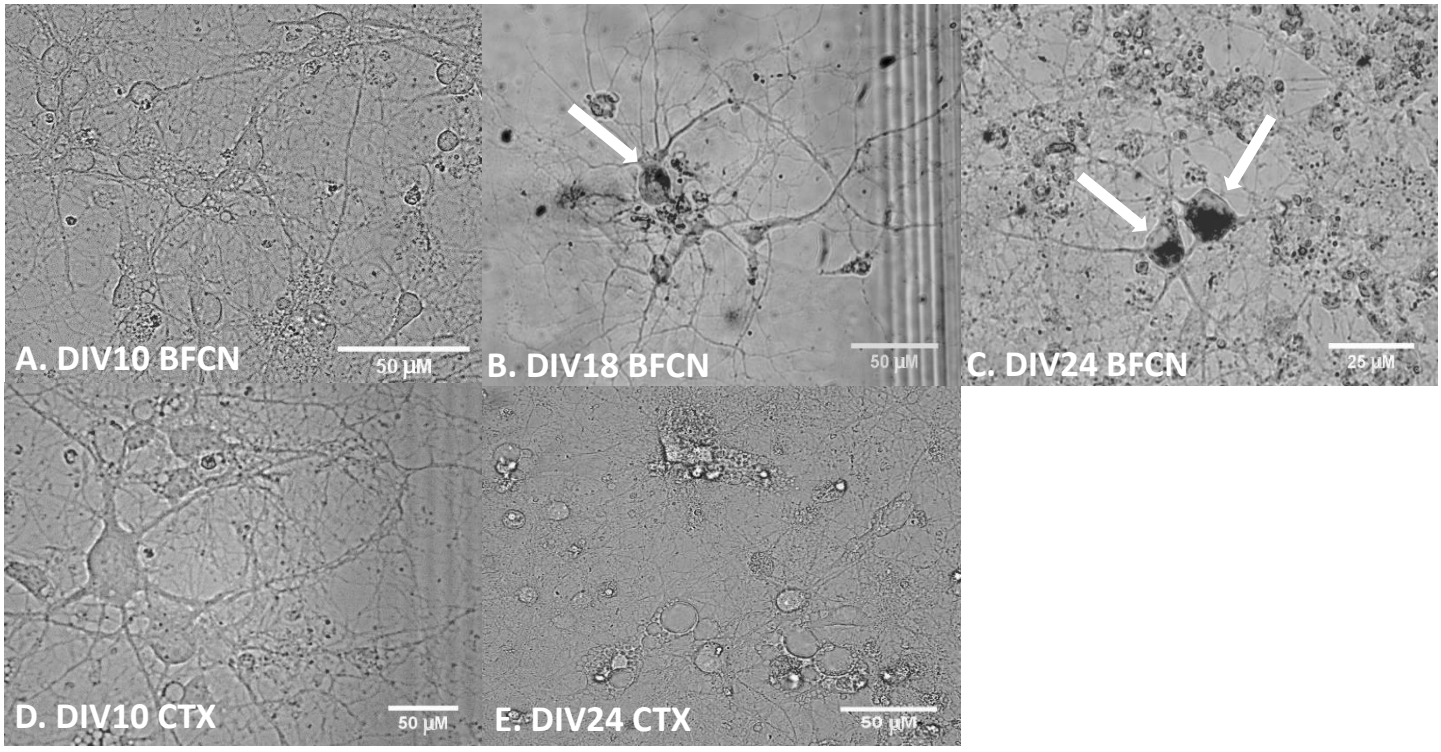

Figure 7.

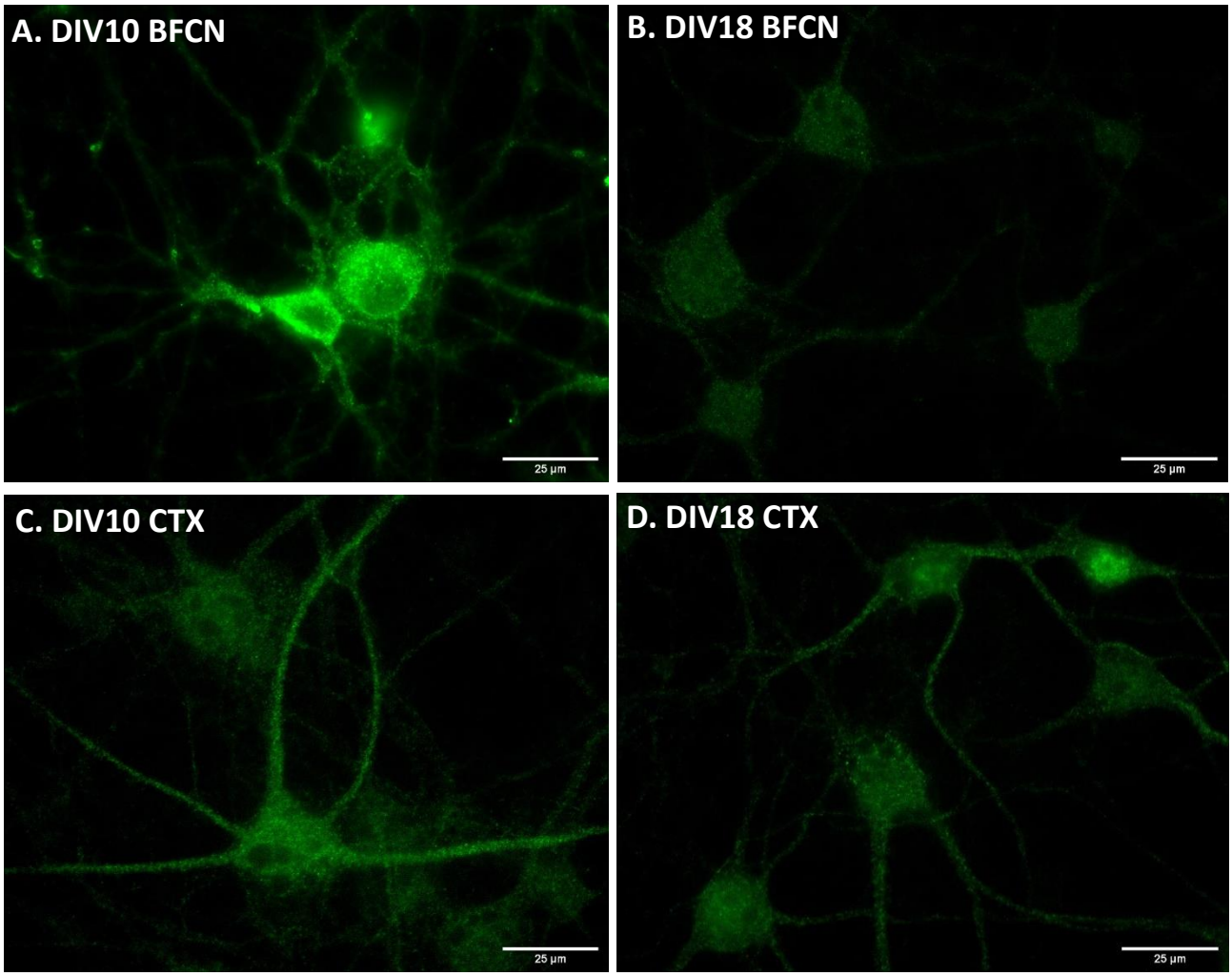
A. DIV10 BFCN
B. DIV18 BFCN
C. DIV10 CTX
D. DIV18 CTX
25 µm

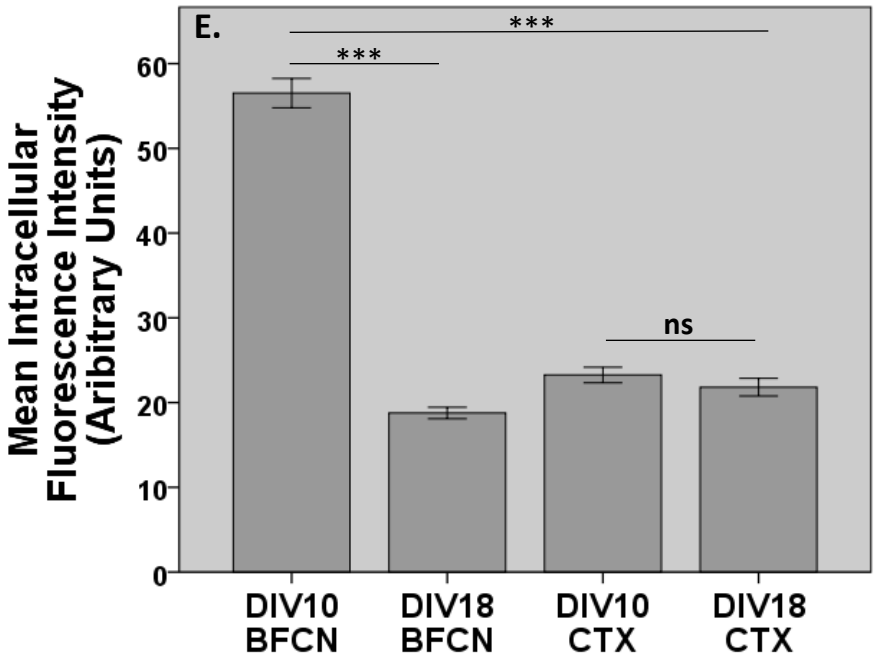
E.
***
***
ns
Mean Intracellular Fluorescence Intensity (Aribitrary Units)
0
10
20
30
40
50
60
DIV10 BFCN
DIV18 BFCN
DIV10 CTX
DIV18 CTX

Figure 8.

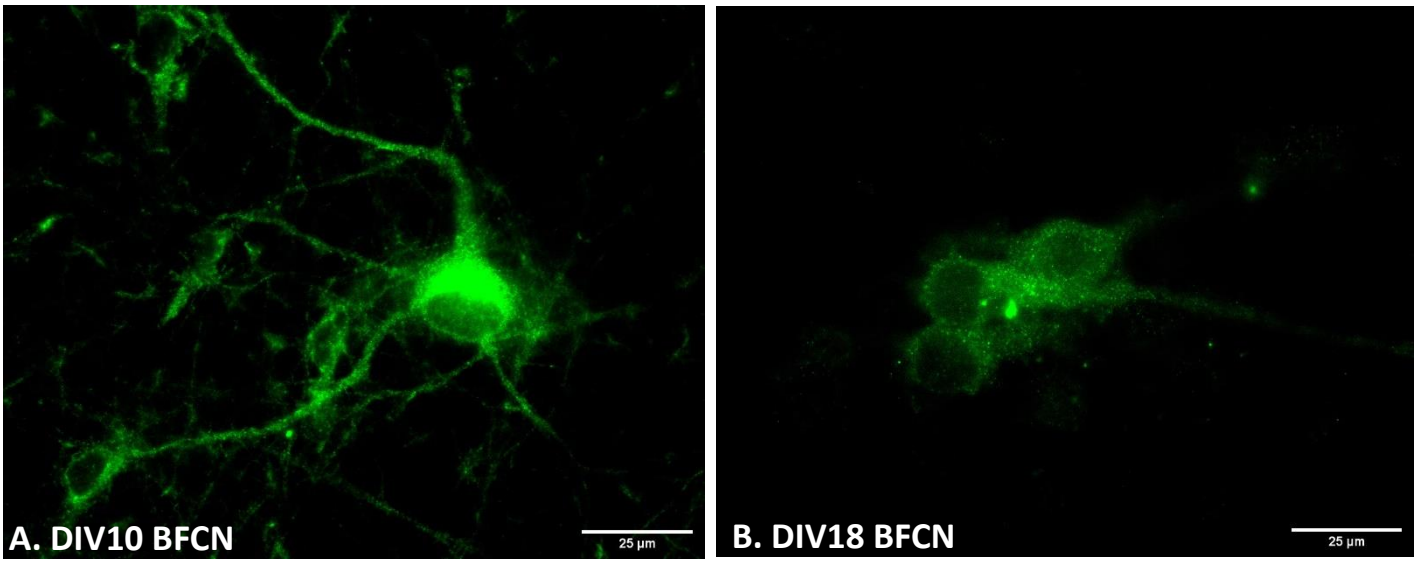
A. DIV10 BFCN
25 µm
B. DIV18 BFCN
25 µm

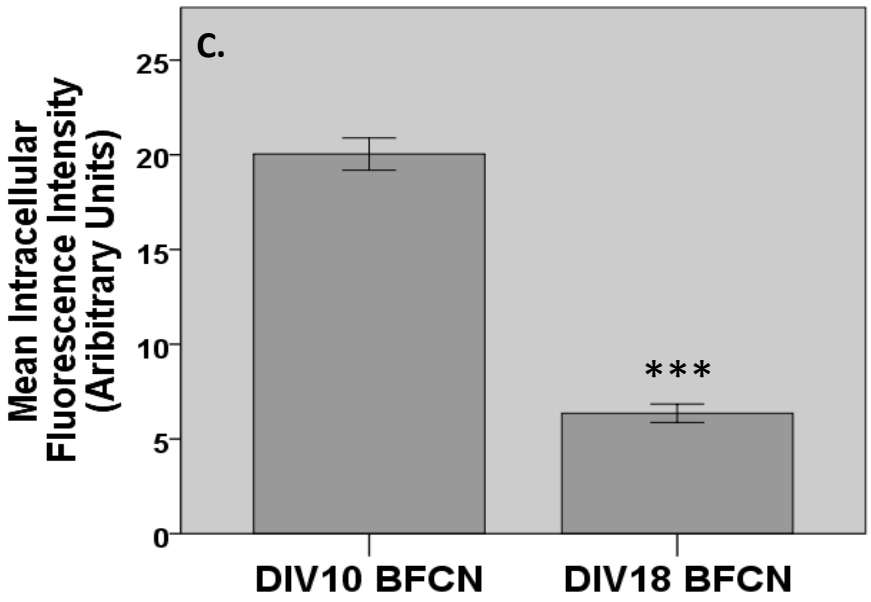
C.
Mean Intracellular Fluorescence Intensity (Aribitrary Units)
25
20
15
10
5
0
***
DIV10 BFCN
DIV18 BFCN

Figure 9.

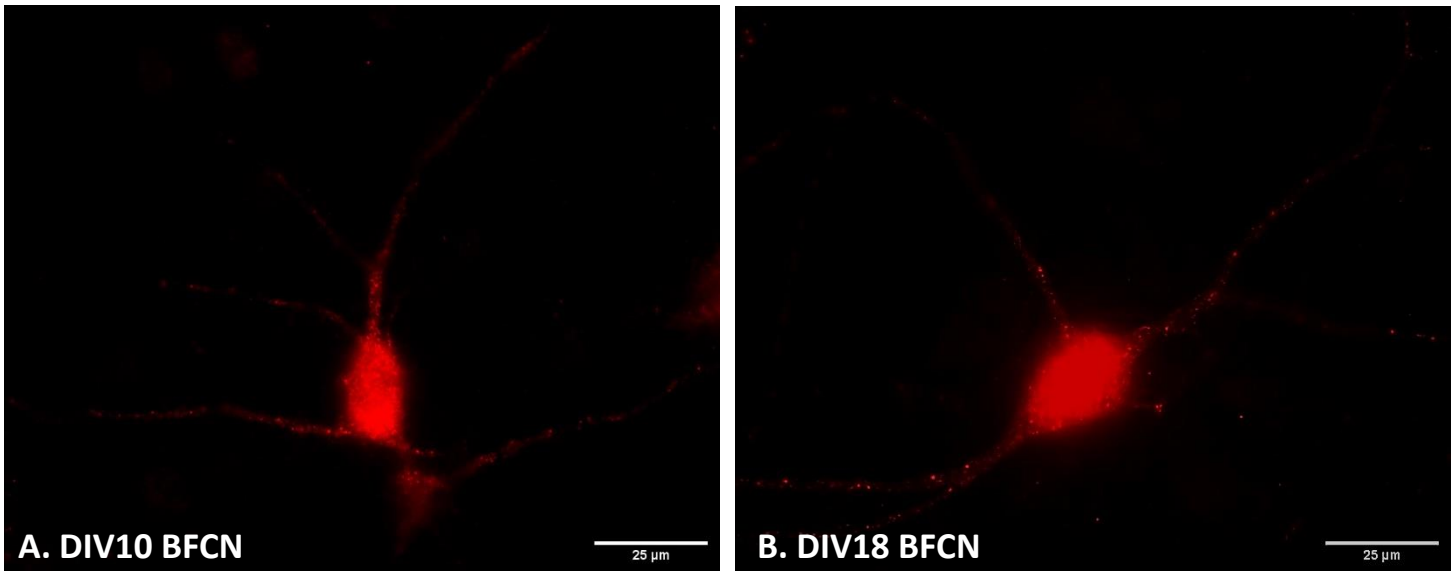
A. DIV10 BFCN
25 µm
B. DIV18 BFCN
25 µm

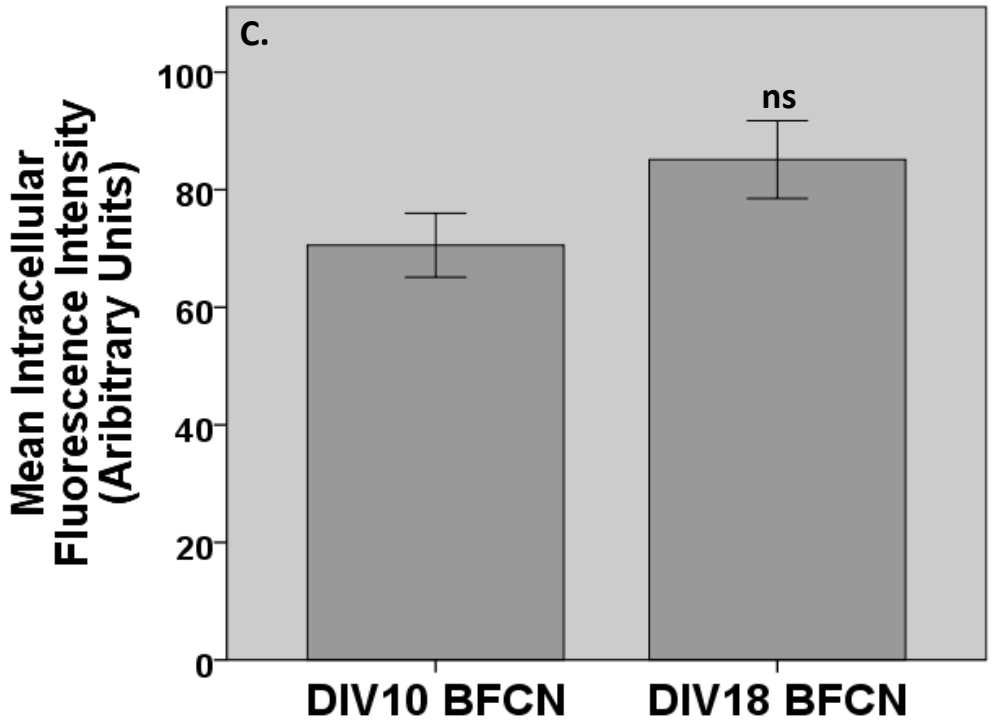
C.
Mean Intracellular Fluorescence Intensity (Aribitrary Units)
100
80
60
40
20
0
ns
DIV10 BFCN
DIV18 BFCN

Supplementary Figure 1.

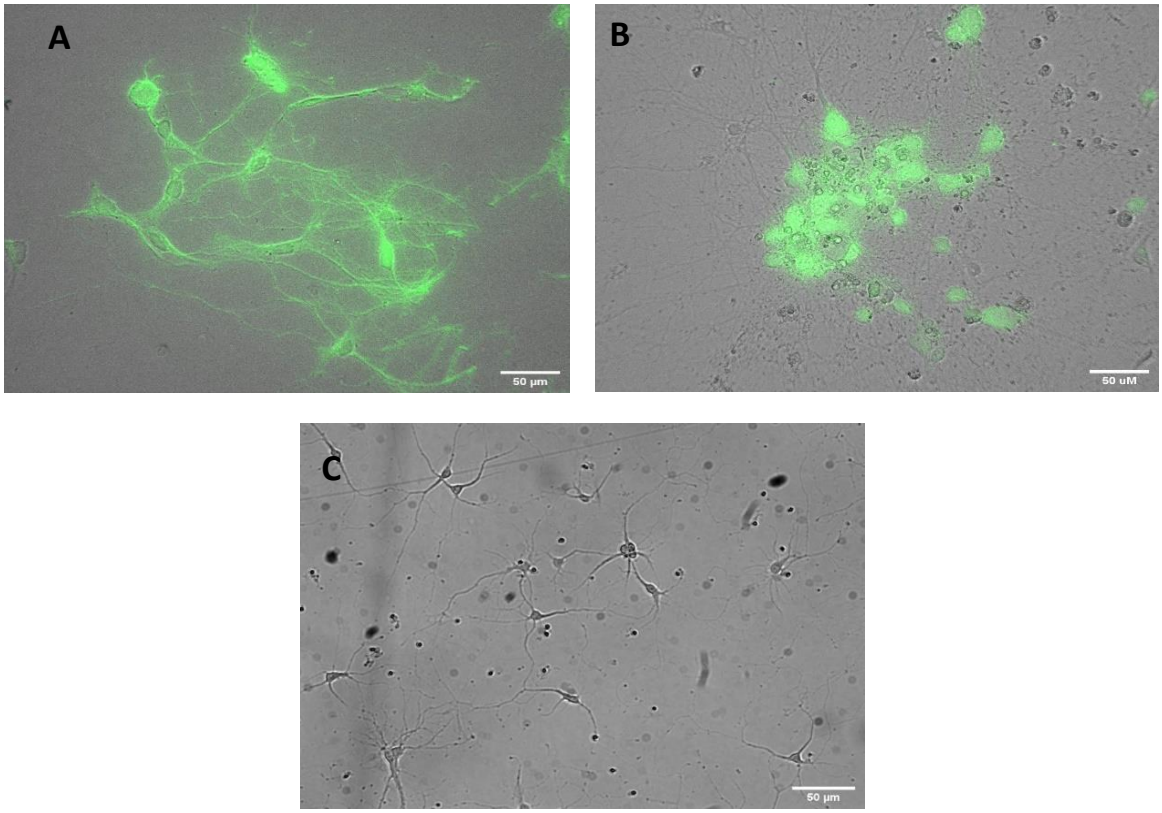

Supplementary Figure 2.

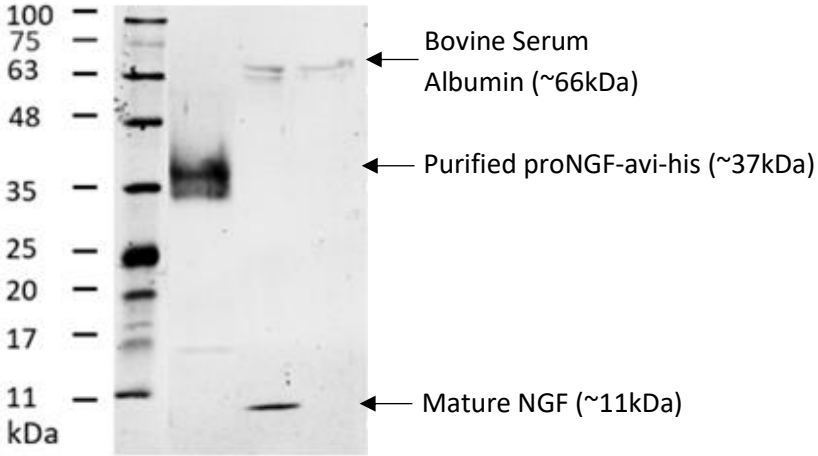

Supplementary Figure 1.

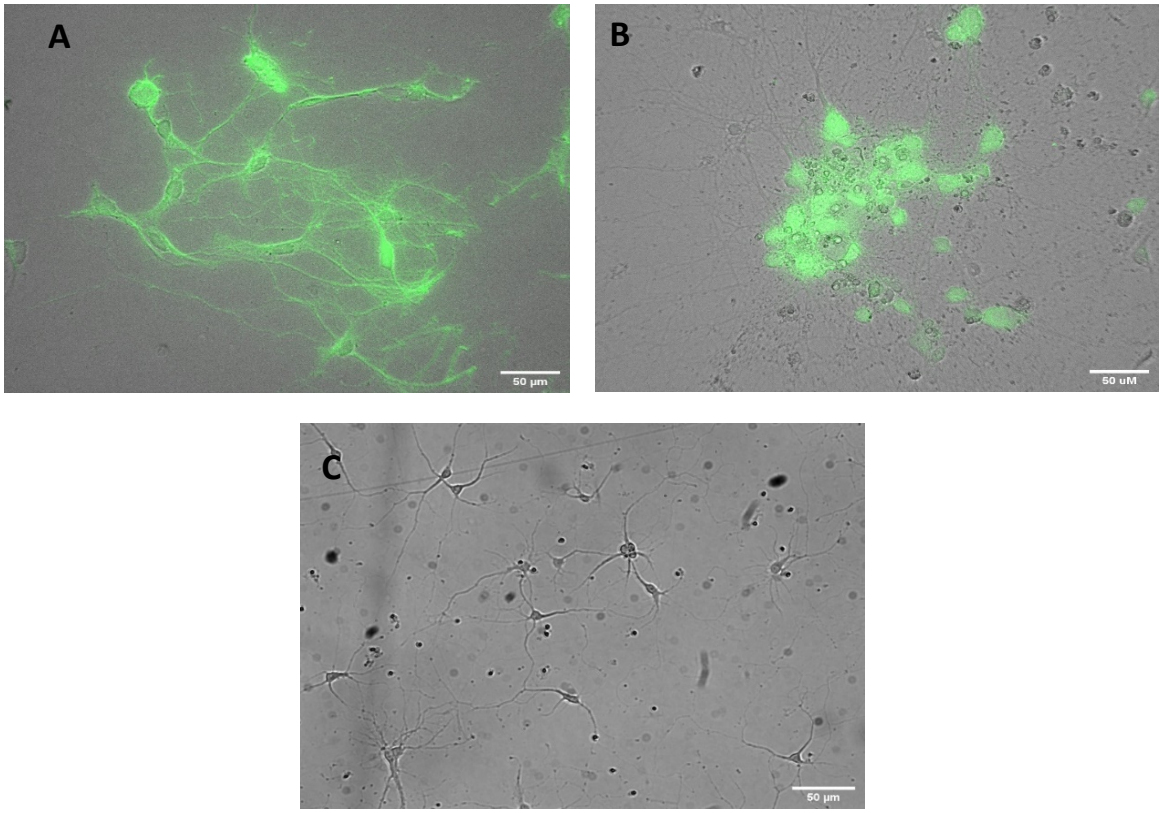

Supplementary Figure 1. TrkA and VAChT Staining in BFCNs. Basal forebrain neurons grown in microfluidic chambers for 10 days stained with an antibody against TrkA (A) and vesicular acetylcholine transporter (B). Cortical neurons did not stain with either marker (C).

Supplementary Figure 2.

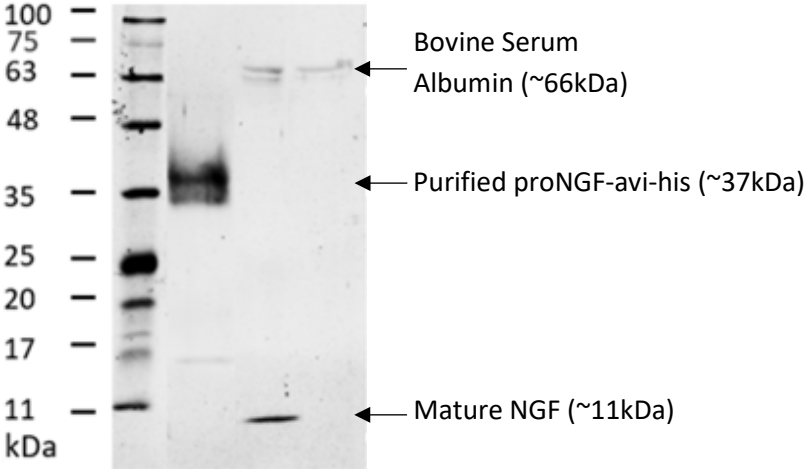

Supplementary Figure 2. Western blot of proNGF purified from HEK cell medium. Blots were completed as described in Fahnestock et al. (2001). Lane 1, 50 pg of nickel-affinity purified protein. Lane 2, 100 pg recombinant mature NGF. Lane 3, elution buffer (no protein). No mature NGF was detected in the purified protein sample.